Histone Deacetylase Inhibitors Interact with Melanoma Differentiation Associated-7/Interleukin-24 to Kill Primary Human Glioblastoma Cells

Hossein A. Hamed, Adly Yacoub, Margaret A. Park, Kellie Archer, Swadesh K. Das, Devanand Sarkar, Steven Grant, Paul B. Fisher, and Paul Dent

Department of Neurosurgery (H.A.H., A.Y., P.D.), Department of Medicine (S.G.), Department of Human and Molecular Genetics (S.K.D., D.S., P.B.F.), Department of Biochemistry and Molecular Biology (M.A.P.), Biostatistics (K.A.), and the VCU Institute of Molecular Medicine (D.S., S.G., P.B.F., P.D.), Virginia Commonwealth University, Richmond, Virginia

ABSTRACT

We presently demonstrate that histone deacetylase inhibitors (HDACIs) enhance toxicity of melanoma differentiation-associated gene-7/interleukin 24 (mda-7/IL-24) in invasive primary human glioblastoma multiforme (GBM) cells. Additionally, a method is described to augment the efficacy of adenoviral delivery of mda-7/IL-24 in these cells. HDACIs synergized with melanoma differentiation-associated (MDA)-7/IL-24 killing GBM cells. Enhanced lethality correlated with increased autophagy that was dependent on the expression of ceramide synthase 6. HDACIs interacted with MDA-7/IL-24 prolonging generation of reactive oxygen species and Ca^{2+}. Quenching of reactive oxygen species and Ca^{2+} blocked HDACI and MDA-7/IL-24 killing. In vivo MDA-7/IL-24 prolonged the survival of animals carrying orthotopic tumors, and HDACIs enhanced survival further. A serotype 5/3 adenovirus more effectively delivers mda-7/IL-24 to GBM tumors than a serotype 5 virus. Hence, we constructed a serotype 5/3 adenovirus that conditionally replicates in tumor cells expressing MDA-7/IL-24, in which the adenoviral early region 1A (E1A) gene was driven by the cancer-specific promoter progression elevated gene-3 [Ad.5/3 (INGN 241)-PEG-E1A-mda-7; also called Ad.5/3-CTV (cancer terminator virus)]. Ad.5/3-CTV increased the survival of mice carrying GBM tumors to a significantly greater extent than did a nonreplicative virus Ad.5/3-mda-7. Ad.5/3-CTV exhibited no toxicity in the brains of Syrian hamsters. Collectively our data demonstrate that HDACIs enhance MDA-7/IL-24 lethality, and adenoviral delivery of mda-7/IL-24 combined with tumor-specific viral replication is an effective preclinical GBM therapeutic.

Introduction

Glioblastoma multiforme (GBM) is diagnosed in ~20,000 patients per annum (Robins et al., 2007). Even under circumstances in which virtually all of the tumor can be surgically removed and the patients are maximally treated with radiation and chemotherapy, the mean survival of this disease is only extended from 3 months to 1 year (Robins et al., 2007).

The mda-7 gene (interleukin 24; IL-24) was isolated from human melanoma cells induced to undergo differentiation by treatment with interferon and mezerein (Jiang et al., 1995). The expression of melanoma differentiation-associated (MDA)-7/IL-24 protein is decreased in advanced melanomas, with almost undetectable levels in metastatic disease (Jiang et al., 1995; Ekmekcioglu et al., 2001; Ellerhorst et al., 2002). Enforced expression of MDA-7/IL-24, by use of a recombinant adenovirus Ad.5-mda-7 (INGN 241) inhibits the growth and kills a broad spectrum of cancer cells without exerting harmful effects in normal human epithelial or fibroblast cells (Su et al., 1998, 2001; Fisher et al., 2003; Fisher, 2005; Lebedeva et al., 2005; Gupta et al., 2006a,b). Mda-7/IL-24 was evaluated in a phase I clinical trial in patients with advanced cancers, which concluded that an Ad.5-mda-7 injected intratumorally was safe; with repeated injections, significant clinical activity was evident (Fisher et al., 2003; Cunningham et al., 2005; Lebedeva et al., 2005).

The ability of MDA-7/IL-24 to modulate cell survival processes in transformed cells has been investigated by our

ABBREVIATIONS: Ad.5-mda-7, INGN 241; BCL-XL, B-cell lymphoma-extra large; c-FLIP-s, cellular FLICE [FADD-like IL-1β-converting enzyme]-inhibitory protein short; CAR, coxsackie and adenovirus receptor; cmv, cytomegalovirus; CRM, cytokine response modifier; CTV, cancer terminator virus; DMEM, Dulbecco's modified Eagle's medium; E1A, adenoviral early region 1A; ER, endoplasmic reticulum; FBS, fetal bovine serum; GBM, glioblastoma multiforme; GFP, green fluorescent protein; GST, glutathione S-transferase; HDACI, histone deacetylase inhibitor; IL, interleukin; LASS, longevity assurance gene; MDA, melanoma differentiation-associated; PBS, phosphate-buffered saline; PEG, progression elevated gene; PERK, PKR-like endoplasmic reticulum kinase; pfu, plaque-forming units; ROS, reactive oxygen species; SAHA, vorinostat (suberoylanilide hydroxamic acid, Zolinza); SBHA, suberohydroxamic acid; TUNEL, terminal deoxynucleotidyl transferase mediated dUTP Nick End Labeling assay.

groups (Yacoub et al., 2008a,b, 2010a; Dash et al., 2010a,b; Dent et al., 2010a,b; Sauane et al., 2010; Bhutia et al., 2011). Prior work in GBM cells using bacterially synthesized glutathione S-transferase (GST)-MDA-7 protein has shown that in the low nanomolar concentration range GST-MDA-7 primarily causes a growth arrest response with little induction of cell killing, whereas at ~20-fold greater concentrations, the cytokine causes profound growth arrest and tumor cell death (Sauane et al., 2010; Yacoub et al., 2010a). Key factors implicated in MDA-7/IL-24 toxicity include Ca^{2+} elevation, ceramide generation, and reactive oxygen species (ROS) production (Sauane et al., 2010; Yacoub et al., 2010a,b). Expression of MDA-7/IL-24 increased the levels of autophagy, and inhibition of autophagy protected against MDA-7/IL-24 toxicity (Yacoub et al., 2008a,b, 2010a).

Many cancer gene therapy studies have used type 5 adenovirus vectors (Curiel and Fisher, 2012). For a type 5 virus to infect a cell requires expression of the coxsackie and adenovirus receptor (CAR); however, CAR is known to be downregulated in many cancer types including GBM (Paul et al., 2008; Curiel and Fisher, 2012). To circumvent the low efficiency of a type 5 adenovirus infection, we created a novel tropism modified vector by replacing the type 5 virus fiber knob with the fiber knob of the type 3 adenovirus, resulting in enhanced infection of tumor cells in a CAR-independent manner; our prior preclinical studies in prostate cancer and GBM provide evidence for the enhanced therapeutic efficacy of Ad.5/3-*mda*-7 versus Ad.5-*mda*-7 (Dash et al., 2010a,b; Hamed et al., 2010). Further studies developed a conditionally replication-competent adenovirus where expression of the adenoviral early region 1A (E1A) virus gene and conditional virus replication was driven by the promoter of progression elevated gene-3 (*PEG-3*), a promoter that is active only in cancer cells such as GBM cells but has little activity in normal cells such as primary astrocytes (Ad.5-PEG-E1A-*mda*-7; a cancer terminator virus, Ad.5-*CTV*) (Su et al., 2005; Sarkar et al., 2007, 2008). Ad.5-*CTV* injected into prostate cancer or melanoma xenografts in athymic mice eradicated not only the primary infected tumor but also an uninfected tumor growing on the opposite flank (Sarkar et al., 2007, 2008). This finding can be explained by the fact that secreted MDA-7/IL-24 protein, generated from cells infected with Ad.5-*mda*-7, induces growth inhibition and apoptosis in surrounding noninfected cancer cells through a "bystander" antitumor effect (Sauane et al., 2008; Emdad et al., 2009).

Histone deacetylase inhibitor (HDACIs) are a structurally diverse class of agents, such as vorinostat [SAHA; suberoylanilide hydroxamic acid; Zolinza (Patheon, Inc., Mississauga, ON, Canada)] and sodium valproate (Depakote; Abbott Laboratories, Abbott Park, IL). These agents block histone deacetylation and neutralization of positively charged lysine residues on histone tails, thereby modifying chromatin structure/condensation and transcription (Ellis and Pili, 2010; Spiegel et al., 2012). The mode of HDACI action is in fact multifactorial, with an additional ~20 targets (Dai et al., 2005; Frew et al., 2009; Tang et al., 2012). We have shown that induction of DNA damage and the generation of ceramide and ROS production is a common mechanism involved in both MDA-7/IL-24 and HDACs-induced antitumor activity. As with MDA-7/IL-24, HDACIs have been shown to have selective toxicity in tumor cells compared with nontransformed cells (Rosato and Grant, 2004).

Our present studies were performed to determine whether MDA-7/IL-24 and HDACIs could interact to kill GBM cells and whether a serotype 5/3 adenovirus that conditionally replicates in tumor cells expressing MDA-7/IL-24 increased the survival of mice carrying GBM tumors to a greater extent than did a nonreplicative virus Ad.5/3-*mda*-7.

Materials and Methods

Suberohydroxamic acid (SBHA) and vorinostat (SAHA) were supplied by Calbiochem (San Diego, CA) as a powder, which we dissolved in sterile dimethylsulfoxide and stored frozen under light-protected conditions at −80°C. Trypsin-EDTA, Dulbecco's modified Eagle's medium (DMEM), RPMI medium, and penicillin-streptomycin were purchased from Gibco BRL (Gibco/Life Technologies, Grand Island, NY). Dr. C. D. James of the University of California at San Francisco very generously originally supplied the primary human GBM cells (GBM6, GBM12, and GBM14) and the information on the genetic background of such cells. Dr. S. Spiegel (Virginia Commonwealth University) supplied the plasmid to express LC3-green fluorescent protein (GFP). Other reagents were of the highest quality commercially available (Sarkar et al., 2008; Yacoub et al., 2008a,b, 2010a).

Methods

Generation of Adenoviruses. Recombinant serotype 5 and serotype 5/3 adenoviruses to express MDA-7/IL-24 and control empty vector were generated as described elsewhere (Dash et al., 2010a,b; Hamed et al., 2010). Ad5/3.PEG-E1.*mda*-7 (Ad.5/3-*CTV*) was prepared in collaboration with Drs. Igor Dmitriev and David Curiel of the Washington University School of Medicine (Saint Louis, MO). This recombinant virus was generated in three consecutive steps. 1) Homologous recombination of pAd5/3 genomic plasmid with pShuttlE3 plasmid containing the *mda*-7/IL-24 expression cassette and kanamycin selection resulted in the pAd5/3.E3-*mda*-7 genome. 2) pAd5/3.E3-*mda*-7 was cut with *Swa* I to excise the kanamycin resistance gene. 3) The resultant pAd5/3.E3-*mda*-7 plasmid was recombined with pShuttlE1 plasmid containing E1A and E1B genes under control of the *PEG-3* promoter, resulting in the Ad5/3.PEG-E1.*mda*-7 (Ad5/3-*CTV*) genomic plasmid. This plasmid was digested with *Pac* I to release viral inverted terminal repeats (ITRs) and transfected in A549 cells to rescue the conditional replication competent adenovirus (CRCA) Ad.5/3-*CTV*. Similar strategies were used to generate Ad.5/3-cytomegalovirus (cmv)-E1A-*mda-7* and Ad.5/3-PEG-*mda*-7. The viruses were expanded and titers determined as previously described elsewhere (Sarkar et al., 2005; Dash et al., 2011; Azab et al., 2012).

Cell Culture and In Vitro Exposure of Cells to GST-MDA-7, "Ad.*mda*-7," and Drugs. All GBM lines were cultured at 37°C [5% (v/v) CO_2] in vitro using RPMI supplemented with 5% (v/v) fetal calf serum and 10% (v/v) nonessential amino acids. For short-term cell-killing assays and immunoblotting, the cells were plated at a density of 3×10^3 per cm^2, and 36 hours after plating were treated with MDA-7/IL-24 and/or various drugs, as indicated. In vitro small molecule inhibitor treatments were from a 100 mM stock solution of each drug, and the maximal concentration of the vehicle (dimethylsulfoxide) in media was 0.02% (v/v). For adenoviral infection, the cells were infected 12 hours after plating, and the expression of the recombinant viral transgene was allowed to occur for at least 12 hours before any additional experimental procedure. Cells were not cultured in reduced serum media during any study.

Recombinant Adenoviral Vectors; Infection In Vitro. We generated and purchased the previously noted recombinant serotype 5 adenoviruses to express dominant negative caspase 9, cellular FLICE [FADD-like IL-1β-converting enzyme]-inhibitory protein short (c-FLIP-s), cytokine response modifier (CRM)-A, and B-cell lymphoma-extra large (BCL-XL) (Vector Biolabs, Philadelphia, PA). Cells were

infected with these adenoviruses at an approximate multiplicity of infection of 50. Cells were incubated for 24 hours to ensure adequate expression of transduced gene products before drug exposures.

Detection of Cell Death by Trypan Blue Assays. Cells were harvested by trypsinization with trypsin/EDTA for ~10 minutes at 37°C. As some apoptotic cells detached from the culture substratum into the medium, these cells were also collected by centrifugation of the medium at 1500g for 5 minutes. The pooled cell pellets were resuspended and mixed with trypan blue dye. Trypan blue stain, in which blue-dye-incorporating cells were scored as being dead, was performed by counting of cells using a light microscope and a hemacytometer. We counted 500 cells from randomly chosen fields; the number of dead cells was counted and expressed as a percentage of the total number of cells counted.

Plasmid Transfection. Plasmid DNA (0.5 μg/total plasmid transfected) was diluted into 50 μl of RPMI growth media that lacked supplementation with fetal bovine serum (FBS) or with penicillin-streptomycin. Lipofectamine 2000 reagent (1 μl) (Invitrogen, Carlsbad, CA) was diluted into 50 μl growth media that lacked supplementation with FBS or with penicillin-streptomycin. The two solutions were then mixed together and incubated at room temperature for 30 minutes. The total mix was added to each well (4-well glass slide or 12-well plate) containing 200 μl growth media that lacked supplementation with FBS or with penicillin-streptomycin. The cells were incubated for 4 hours at 37°C, after which time the media was replaced with RPMI growth media containing 5% (v/v) FBS and 1× penicillin-streptomycin.

Microscopy for LC3-GFP Expression. Where indicated, the LC3-GFP transfected cells were 12 hours after transfection infected with either "Ad.*cmv*" or "Ad.*mda-7*" then cultured for 24 hours. LC3-GFP transfected cells were visualized at the indicated time points on the Zeiss Axiovert 200 microscope (Carl Zeiss Light Microscopy, Göttingen, Germany) using the fluorescein isothiocyanate filter.

Intracerebral Inoculation of GBM Cells. Athymic female NCr-nu/nu mice (National Cancer Institute, Frederick National Laboratory, Frederick, MD) weighing ~20 g, were used for this study. The mice were maintained under pathogen-free conditions in facilities approved by the American Association for Accreditation of Laboratory Animal Care and in accordance with current regulations and standards of the U.S. Department of Agriculture, Washington, DC, the U.S. Department of Health and Human Services, Washington, DC, and the National Institutes of Health, Bethesda, MD. GBM cells were cultured in DMEM supplemented with 5% (v/v) fetal calf serum and 100 μg/ml (1% v/v) penicillin-streptomycin. Cells were incubated in a humidified atmosphere of 5% (v/v) CO_2 at 37°C.

The mice were anesthetized via i.p. administration of (ketamine, 40 mg/kg; xylazine, 3 mg/kg) and immobilized in a stereotactic frame. A 24-gauge needle attached to a Hamilton syringe was inserted into the right basal ganglia to a depth of 3.5-mm and then withdrawn 0.5-mm to make space for tumor cell accumulation. The entry point at the skull was 2-mm lateral and 1-mm dorsal to the bregma. Intracerebral injection of 0.5×10^6 glioma cells (~40 mice per cell line per separate experiment) in 2 μl of DMEM medium was performed over 10 minutes. The skull opening was enclosed with sterile bone wax, and the skin incision was closed using sterile surgical staples.

Adenoviral vectors were administered 7 days after tumor cell implantation via stereotactic injection into the intracerebral tumor using the same anesthesia procedure and stereotactic frame coordinates described previously. Viral vectors suspended in 2 μl of phosphate-buffered saline (PBS) were delivered by slow infusion over a 6-minute period.

Immunohistochemistry and Staining of Fixed Tumor Sections. After sacrifice, the tumors and associated mouse brains were fixed in optimum cutting temperature (O.C.T.) compound (Tissue-Tek; Sakura Finetek USA, Torrance, CA); cryostat sectioned (Leica Biosystems, Buffalo Grove, IL) as 12 μm sections. Nonspecific binding was blocked with a 2% (v/v) rat sera, 1% (v/v) bovine sera, 0.1% (v/v) Triton ×100, 0.05% (v/v) Tween-20 solution, then sections were stained for cell-signaling pathway markers. For staining of sectioned tumors, primary antibodies were applied overnight, sections washed with a phosphate buffer solution, and secondary antibodies applied for detection (as indicated in the figures): goat anti-rat Alexa 488/647 (1:500; Invitrogen), and goat anti-mouse Alexa 488/647 (1:500; Invitrogen) secondary antibody as per the primary antibody used as per the manufacturer's instructions. Sections were then dehydrated, cleared, and mounted with cover-slips using Permount (Fisher Scientific, Hampton, NH). Apoptotic cells with double-stranded DNA breaks were detected using the Upstate TUNEL (terminal deoxynucleotidyl transferase mediated dUTP Nick End Labeling assay) Apototic Detection Kit (EMD Millipore, Billerica, MA) according to the manufacturer's instructions. Slides were applied to high-powered light/confocal microscopes (Zeiss LSM 510 Meta-confocal scanning microscope; Zeiss HBO 100 microscope with Axio Cam MRm camera; Carl Zeiss Light Microscopy) at the magnification indicated in the figure legends. Data shown are representative slides from several sections from the same tumor with multiple tumors (from multiple animals and multiple experiments) having been examined (n = at least 3–8 animals-tumors).

Data Analysis. Comparison of the effects of various treatments was performed using one-way analysis of variance and a two-tailed Student's t test. $P < 0.05$ was considered statistically significant. Statistical examination of the in vivo animal survival data used log rank statistical analyses between the different treatment groups. Experiments shown are the mean of multiple individual points from multiple experiments ($\pm$ S.E.M.).

Results

We determined whether HDACIs enhanced MDA-/IL-24 toxicity in primary human GBM cells. GBM6, GBM12, and primary human astrocytes were infected with empty vector serotype 5 adenovirus (Ad.5-*cmv*) or a virus to express MDA-7/IL-24 (Ad.5-*mda*-7). Use of serotype 5 recombinant adenoviruses has been widespread for in vitro use as well as clinically. Twelve hours after the infection, the cells were treated with increasing doses of the HDACIs, sodium valproate, or SBHA. In a dose-dependent fashion, the treatment with HDACIs enhanced the lethality of MDA-7/IL-24 in GBM cells but not in primary human astrocytes (Fig. 1, A–C). Results for the drug alone, without infection of the control virus, were identical to those in control virus–infected cells (unpublished data). In the colony-formation assays, both valproate and SBHA synergized with MDA-7/IL-24 protein to kill GBM cells (Table 1).

In a time-dependent fashion, MDA-7/IL-24 protein increased autophagy (LC3-GFP vesicle) levels in GBM cells (Fig. 2A). SBHA enhanced the MDA-7/IL-24–stimulated autophagy levels, and knock down of Beclin1 abolished autophagy. Knock down of Beclin1 suppressed both MDA-7/IL-24 and MDA-7/IL-24 plus SBHA toxicity (Fig. 2B). MDA-7/IL-24 protein and SBHA interacted in a greater than additive fashion to activate PKR-like endoplasmic reticulum kinase (PERK) and to increase phosphorylation of the downstream substrate of PERK, eIF2α (Fig. 2C). Expression of dominant negative PERK suppressed the induction of autophagy and suppressed killing by the combination of agents (Fig. 2, D and E).

Ceramide generation plays a key role in MDA-7/IL-24 lethality, with activation of the de novo ceramide synthesis pathway (ceramide synthase 6 [LASS6; longevity assurance gene]) playing a key role in MDA-7/IL-24–induced ROS levels and changes in cytosolic Ca^{2+} (Yacoub et al., 2010a). Knock down of LASS6 expression suppressed the induction of
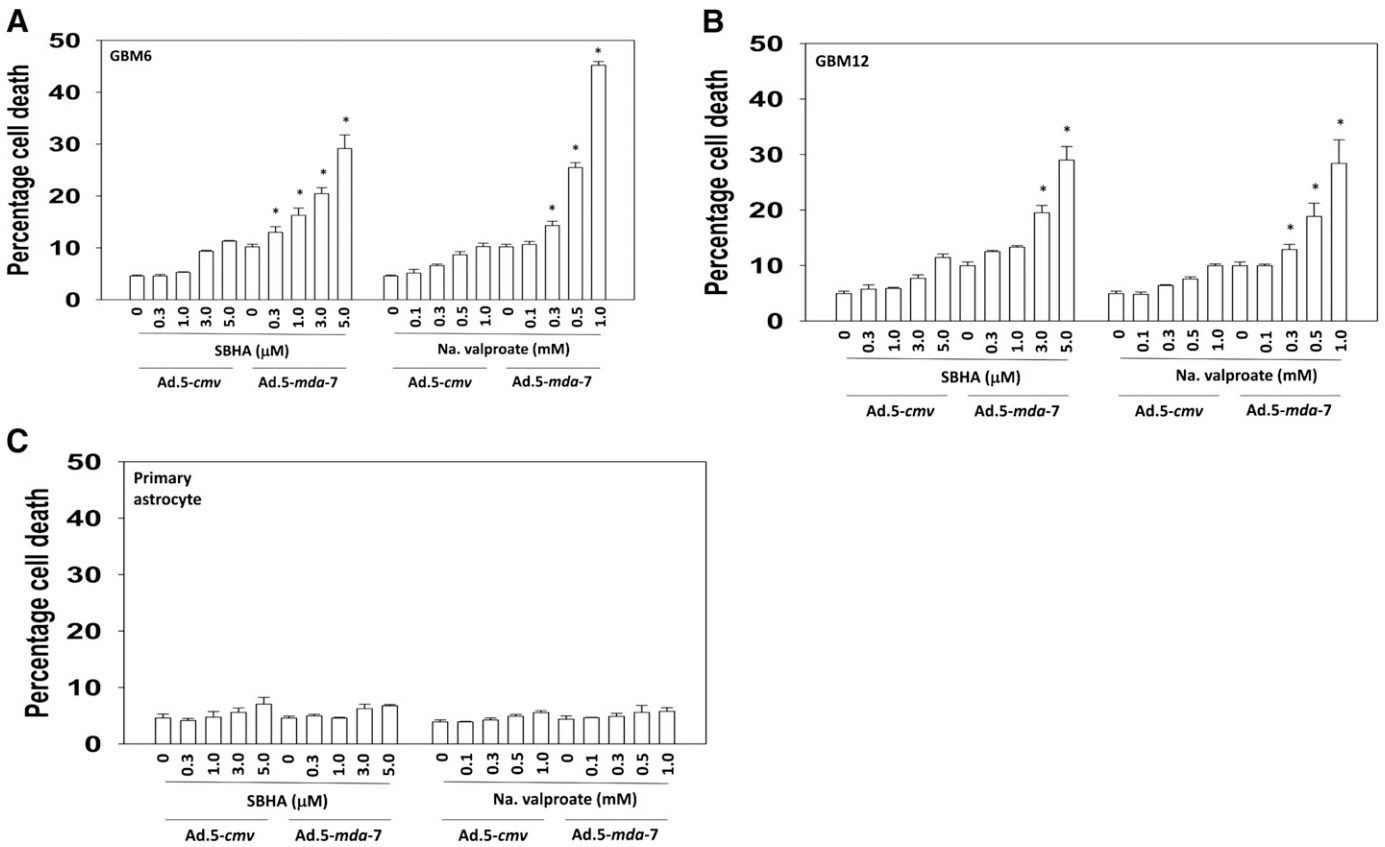
Fig. 1. SBHA and sodium valproate (Na Val) enhance Ad.5-*mda*-7 toxicity in multiple primary human GBM isolates but not in primary human astrocytes. (A) GBM6 cells, (B) GBM12 cells, and (C) primary human astrocytes were infected with empty vector or recombinant serotype 5 adenovirus to express MDA-7/IL-24 at a multiplicity of infection (moi) of 10. After infection (24 hours), cells were treated with vehicle control or with pharmacologically achievable concentrations of HDACIs, sodium valproate (Na Val: 0, 0.3, 0.5, 1.0 mM), or the vorinostat analog SBHA (0, 0.3, 1.0, 3.0, 5.0 μM). Cells were isolated 48 hours later, and viability was determined by trypan blue exclusion ($n = 3$, $\pm$ S.E.M.). *$P < 0.05$ greater than corresponding value in Ad.5-*cmv*-infected cells.

autophagy in GBM cells and suppressed killing by the combination of Ad.5-*mda*-7 and SBHA (Fig. 3, A and B).

We next determined the roles of ROS and changes in cytosolic Ca^{2+} in the response of GBM cells to MDA-7/IL-24 and HDACIs. Ad.5-*mda*-7 and SBHA interacted in a greater than additive fashion to increase ROS and Ca^{2+} levels (Fig. 4, A and B). HDACI treatment: 1) increased the initial Ad.5-*mda*-7–induced ROS and Ca^{2+} levels, and 2) prolonged the increase in ROS and Ca^{2+} signaling. Quenching of ROS-expressing thioredoxin or quenching of Ca^{2+} using calbindin

suppressed MDA-7/IL-24 and MDA-7/IL-24 plus SBHA toxicity (Fig. 4C).

GBM cells were infected to express c-FLIP-s and CRM-A (inhibitors of the extrinsic apoptosis pathway) or infected to express BCL-XL and dominant negative caspase 9 (inhibitors of the intrinsic apoptosis pathway). Expression of c-FLIP-s or CRM-A did not alter MDA-7/IL-24 toxicity as a single agent (Fig. 5A). However, expression of c-FLIP-s or CRM-A suppressed the ability of SBHA to enhance MDA-7/IL-24 toxicity. Expression of BCL-XL or dominant negative caspase 9 suppressed MDA-7/IL-24 and MDA-7/IL-24 plus SBHA toxicity. We determined whether inhibitors of protective BCL-2 family proteins enhanced killing by MDA-7/IL-24. Treatment of GBM cells with either the BCL-2/BCL-XL/MCL-1 inhibitor obatoclax or the BCL-2/BCL-XL inhibitor HA14-1 enhanced the lethality of Ad.5-*mda*-7 (Fig. 5B). These data are similar to prior studies in prostate cancer cells using the BCL-2 family inhibitor sabutoclax (Dash et al., 2011; Azab et al., 2012).

We developed a tropism modified recombinant adenovirus to express MDA-7/IL-24 that comprises the tail and shaft domains of a serotype 5 adenovirus and the knob domain of a serotype 3 virus (Dash et al., 2010a,b; Hamed et al., 2010). We have published that Ad.5/3-*mda*-7 prolonged the survival of animals carrying GBM tumors to a greater extent than did Ad.5-*mda*-7 (Hamed et al., 2010). GBM cells were implanted

TABLE 1
MDA-7/IL-24 synergizes with HDACIs to kill primary human GBM cells

GBM6 cells were plated as single cells (500–2500 per 60-mm dish, in sextuplicate). Twelve hours after plating, the cells were treated with GST or GST-MDA-7 (10–30 nM), SBHA (1–3 μM), or sodium valproate (Na Val, 0.5–1.5 mM), as indicated. Forty-eight hours later, the cells were washed free of drugs, and the colonies were permitted to form for 20 days ($n = 3 \pm$ S.E.M.). Using the Calcusyn for Windows program, we calculated the fraction affected (Fa) and the combination index (CI). A CI value of less than 1.00 indicates a synergy of interaction.

| GST-MDA-7	SBHA			GST-MDA-7	Na Val		
		Fa	CI			Fa	CI
nM	*μM*			*nM*	*mM*		
10	1	0.36	0.55	10	0.5	0.29	0.46
20	2	0.60	0.50	20	1.0	0.40	0.46
30	3	0.81	0.41	30	1.5	0.49	0.37
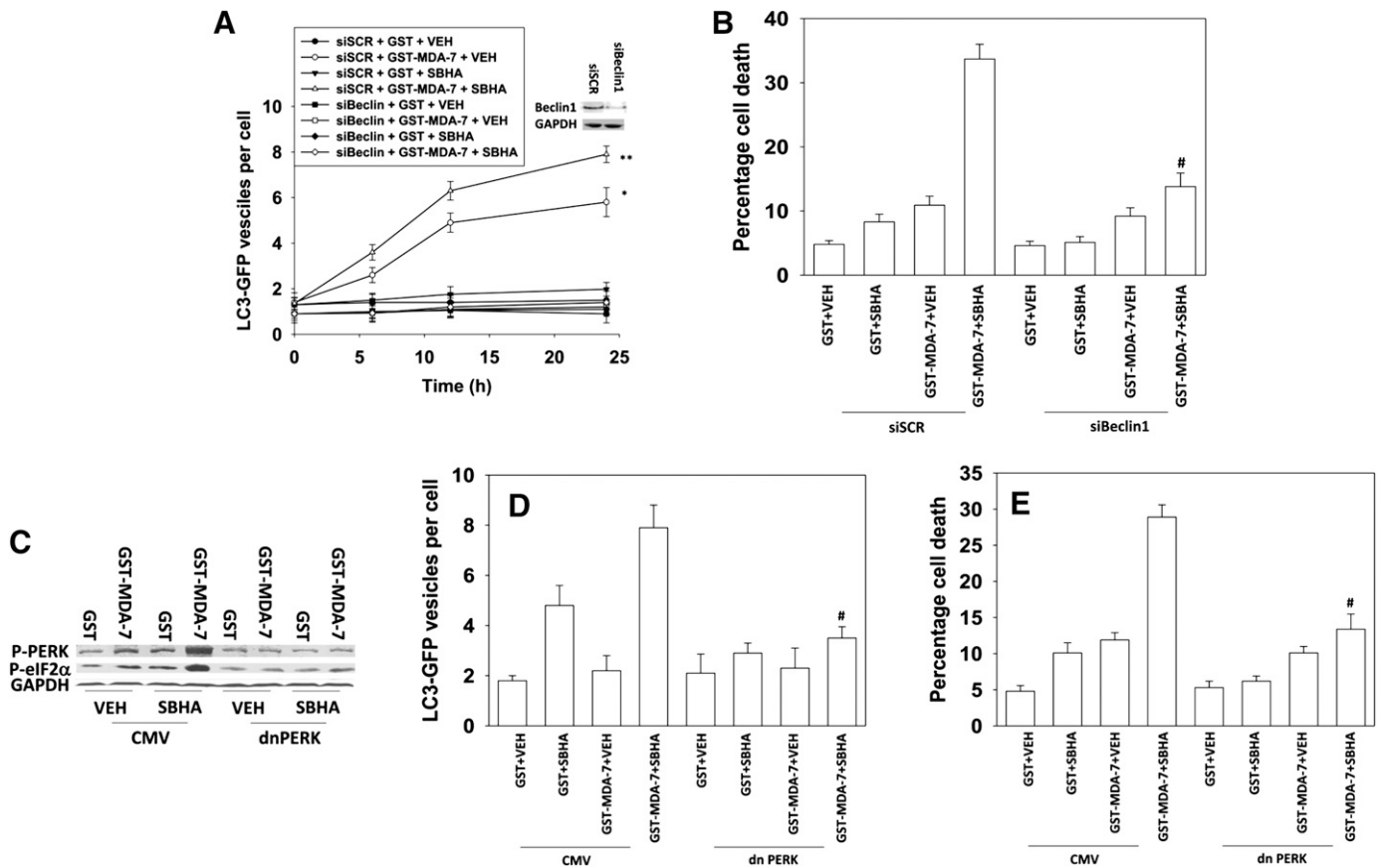
Fig. 2. Induction of ER stress and autophagy plays a role in the interaction between MDA-7/IL-24 and HDACIs. (A) GBM6 cells were transfected in quadruplicate with a plasmid to express an LC3 (ATG8)–GFP fusion protein and in parallel transfected with scrambled small interfering RNA (siRNA; siSCR) or an siRNA to knock down Beclin1 expression. Twenty-four hours after transfection, the cells were treated with GST or GST-MDA-7 (20 nM) and/or SBHA (3 μM). Cells (a representative of 40 per well per time point) were examined 6, 12, and 24 hours after treatment using an Axiovert microscope (40×) for the formation of punctate vesicles containing LC3-GFP. Data are plotted as the number of LC3-GFP vesicles per cell ($n = 2$, ± S.E.M.). *$P < 0.05$ greater than GST + VEH (vehicle); **$P < 0.05$ greater than GST-MDA-7 + VEH (vehicle). (B) GBM6 cells were transfected with siSCR or an siRNA to knock down Beclin1 expression. Twenty-four hours after transfection, the cells were treated with GST or GST-MDA-7 (20 nM) and/or SBHA (3 μM). Cells were isolated 48 hours later, and viability was determined by trypan blue exclusion ($n = 3$, ± S.E.M.). #$P < 0.05$ less than corresponding value in siSCR cells. (C) GBM6 cells were transfected with an empty vector control plasmid or a plasmid to express dominant negative (dn) PERK. Twenty-four hours after transfection, the cells were treated with GST-MDA-7 (20 nM), SBHA (3 μM), or the agents combined. Cells were isolated 6 hours after exposure, and the phosphorylation of PERK and eIF2α determined (representative $n = 2$). (D) GBM6 cells were transfected in quadruplicate with an LC3 (ATG8)–GFP fusion protein and in parallel transfected with an empty vector control plasmid or a plasmid to express dominant negative PERK. Twenty-four hours after transfection, the cells were treated with GST or GST-MDA-7 (20 nM) and/or SBHA (3 μM). Cells (a representative of 40 per well per time point) were examined 24 hours after treatment using an Axiovert microscope (40×) for the formation of punctate vesicles containing LC3-GFP. Data are plotted as the number of LC3-GFP vesicles per cell ($n = 3$, ± S.E.M.). #$P < 0.05$ less than corresponding value in CMV cells. (E) GBM6 cells were transfected with an empty vector control plasmid or a plasmid to express dominant negative PERK. Twenty-four hours after transfection, the cells were treated with GST-MDA-7 (20 nM), SBHA (3 μM), or the agents combined. Cells were isolated 48 hours later, and viability was determined by trypan blue exclusion ($n = 3$, ± S.E.M.). #$P < 0.05$ less than corresponding value in CMV cells.

into the brains of athymic mice and tumors infused with virus. In agreement with our prior publications, infusion of tumors with Ad.5/3-*mda*-7 prolonged animal survival (Fig. 6). Treatment of animals with SAHA did not significantly enhance animal survival. Combined treatment with Ad.5/3-*mda*-7 and SAHA prolonged survival to a significantly greater extent than Ad.5.3-*mda*-7 alone. Collectively our data argue that HDACIs and MDA-7/IL-24 interact to kill GBM cells in vitro and in vivo.

In parallel studies, we generated a serotype 5/serotype 3 recombinant adenovirus to express MDA-7/IL-24 that also conditionally replicates only in tumor cells (Ad.5/3-PEG-E1A-*mda*-7; also known as Ad.5/3-*CTV* in the figures) (see also Sarkar et al., 2007, 2008). We compared the growth suppressive effects of Ad.5/3-*mda*-7 and Ad.5/3-PEG-E1A-*mda*-7 (Ad.5/3-*CTV*) after infection of orthotopic GBM tumors. GBM6 cells stably transfected to express luciferase were implanted

into athymic nude mouse brains. Seven days after implantation, the mice received a single low-dose intratumor infusion of recombinant adenovirus. The viruses infused were Ad.5/3-*cmv* (empty vector control, nonreplicative), Ad.5/3-*PEG-E1A* (empty vector control, tumor selective replication), Ad.5/3-*mda*-7 (MDA-7/IL-24 expression, nonreplicative), and Ad.5/3-*PEG-E1A-mda*-7 (Ad.5/3-*CTV*; MDA-7/IL-24 expression, tumor selective replication). Although a trend was evident, at the low doses of virus used in this study neither Ad.5/3-*PEG-E1A* nor Ad.5/3-*mda*-7 caused a significant decrease in tumor luminosity using a Xenogen IVIS system (i.e., tumor growth) (Fig. 7A). However, infusion of Ad.5/3-*PEG-E1A-mda*-7 (Ad.5/3-*CTV*) resulted in a significant suppression of tumor mass below the initial value.

Animals carrying GBM6-luc tumors were sacrificed, their brains isolated, and immunohistochemistry performed on the
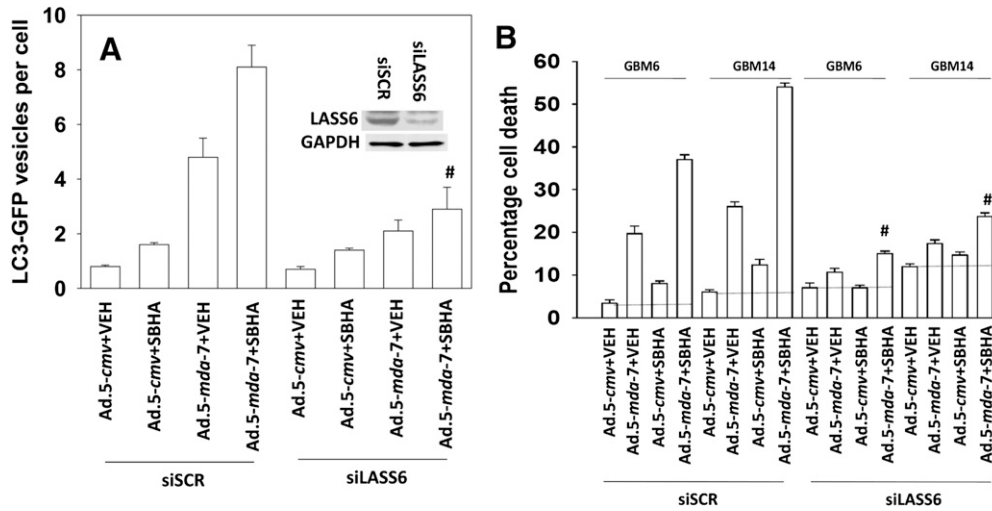
Fig. 3. De novo ceramide generation plays an essential role in the interaction between MDA-7/IL-24 and HDACIs. (A) GBM6 cells were transfected in quadruplicate with a plasmid to express an LC3 (ATG8)–GFP fusion protein and in parallel transfected with scrambled small interfering RNA (siRNA; siSCR) or an siRNA to knock down ceramide synthase 6 (LASS6) expression. Cells were infected with empty vector or recombinant serotype 5 adenovirus to express MDA-7/IL-24; at a multiplicity of infection (moi) of 10. After infection (24 hours), cells were treated with vehicle control or with the vorinostat analog SBHA (3.0 μM). Cells (a representative of 40 per well per time point) were examined 24 hours after treatment using an Axiovert microscope (40$\times$) for the formation of punctate vesicles containing LC3-GFP. Data are plotted as the number of LC3-GFP vesicles per cell ($n = 3$, $\pm$ S.E.M.). $^{\#}P < 0.05$ less than corresponding value in siSCR cells. (B) GBM6 and GBM14 cells were transfected with siSCR or an siRNA to knock down ceramide synthase 6 (LASS6) expression. Twenty-four hours later cells were infected with empty vector or recombinant serotype 5 adenovirus to express MDA-7/IL-24 at an moi of 10. After infection (24 hours), cells were treated with vehicle control or with the vorinostat analog SBHA (3.0 μM). Cells were isolated 48 hours later, and viability was determined by trypan blue exclusion ($n = 3$, $\pm$ S.E.M.). $^{\#}P < 0.05$ less than corresponding value in siSCR cells. GAPDH, glyceraldehyde 3-phosphate dehydrogenase.

GBM6 tumors within brain sections. Ad.5/3-*PEG-E1A* caused a modest enhancement in apoptosis/TUNEL positivity in the tumor, an effect that was considerably greater in Ad.5/3-*mda*-7–infected tumors (Fig. 7B). Ad.5/3-*PEG-E1A-mda*-7–infected tumors had greater levels of TUNEL positivity than Ad.5/3-*mda*-7–infected tumors. In sections of normal brain, no TUNEL staining was evident. Infection of tumors with Ad.5/3-*PEG-E1A* or Ad.5/3-*PEG-E1A-mda*-7 increased E1A immunoreactivity in tumor sections but not in sections of normal brain. This would suggest viral replication and cell killing by Ad.5/3-*PEG-E1A-mda*-7 is restricted to tumor tissue.

We next determined using different doses of adenovirus whether Ad.5/3-PEG-E1A-*mda*-7 was a more efficacious virus at prolonging animal survival when compared with Ad.5/3-PEG-E1A or Ad.5/3-*mda*-7. At the lowest dose of Ad.5/3-PEG-E1A-*mda*-7 tested [1×10^8 plaque-forming units (pfu)], the virus prolonged survival to a greater extent than did infusion of 1×10^9 pfu of Ad.5/3-*mda*-7 (Fig. 7C). The intermediate dose of Ad.5/3-PEG-E1A-*mda*-7 tested (3×10^8 pfu) prolonged survival to a greater extent than did infusion of 1×10^8 pfu of the same virus. Accordingly, infusion of 1×10^9 pfu of Ad.5/3-PEG-E1A-*mda*-7 prolonged survival to a greater extent than did infusion of 3×10^8 pfu of the same virus, with some animals living for >250 days.

Because Ad.5/3-PEG-E1A-*mda*-7 had prolonged animal survival, we performed preliminary toxicology testing of this virus in preparation for its translation into the clinical environment. Syrian hamsters are a U.S. Food and Drug Administration–approved model for oncolytic adenovirus toxicology testing; they are immunocompetent, and they permit human adenovirus replication in normal tissues (Curiel and Fisher, 2012; Dhar et al., 2012). Hamster brains were infused with PBS, an adenovirus that constitutively replicates

Ad.5/3-*cmv*-E1A (3×10^9 pfu), or Ad.5/3-PEG-E1A-*mda*-7 (3×10^9 pfu). Infusion of Ad.5/3-*cmv*-E1A strongly increased the levels of TUNEL positivity and expression of the viral protein E1A in hamster brains (Fig. 7D). Low levels of TUNEL positivity and E1A staining were also evident in the livers of animals who had been infused with Ad.5/3-*cmv*-E1A; no staining of the kidneys was observed. In contrast, infection of hamster brains with Ad.5/3-PEG-E1A-*mda*-7 did not increase TUNEL positivity or E1A levels. Staining for MDA-7/IL-24 protein was evident in Ad.5/3-PEG-E1A-*mda*-7–infected brains. During our studies, we noted that animals infused with Ad.5/3-*cmv*-E1A had enlarged neck lymph nodes, indicative that this virus was generating an immune response (Fig. 7E). In contrast, the lymph nodes of animals infused with PBS or with Ad.5/3-PEG-E1A-*mda*-7 looked identical (and small).

Collectively our in vivo data with Ad.5/3-PEG-E1A-*mda*-7 indicate that the virus significantly prolongs animal survival and has an apparent safe toxicology profile in Syrian hamsters.

Discussion

The research described in this manuscript has focused on developing novel therapies for GBM. To achieve these objectives, we used *mda*-7/IL-24, which has demonstrated tumor cell–specific killing and radiosensitization of glioma cells (Yacoub et al., 2008a,b,c, 2010a). Prior studies have shown that inhibition of signaling pathways can enhance MDA-7/IL-24 toxicity in GBM cells, and our present analyses extended our combinatorial approaches targeting histone deacetylases (Yacoub et al., 2008b; Hamed et al., 2010). We show that HDACIs increase MDA-7/IL-24 toxicity, and we also identify a means of enhancing the therapeutic delivery of MDA-7/IL-24
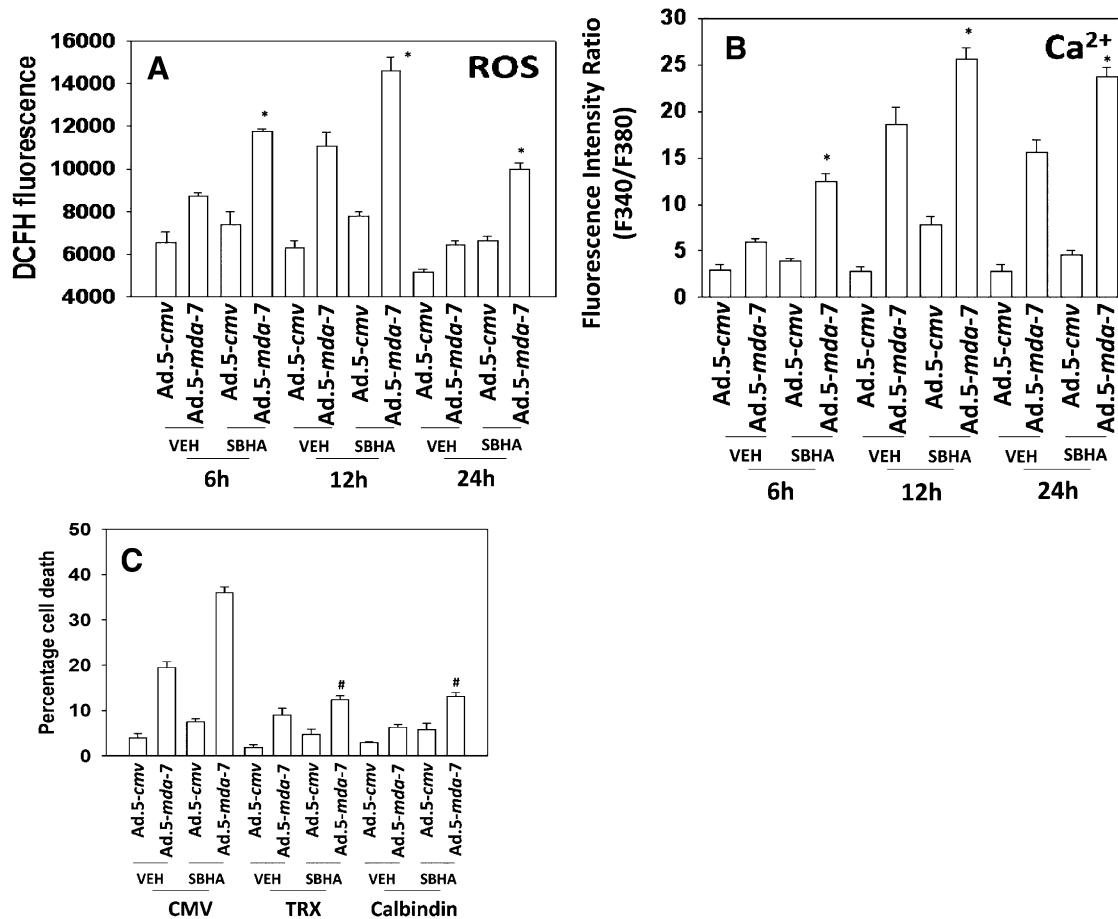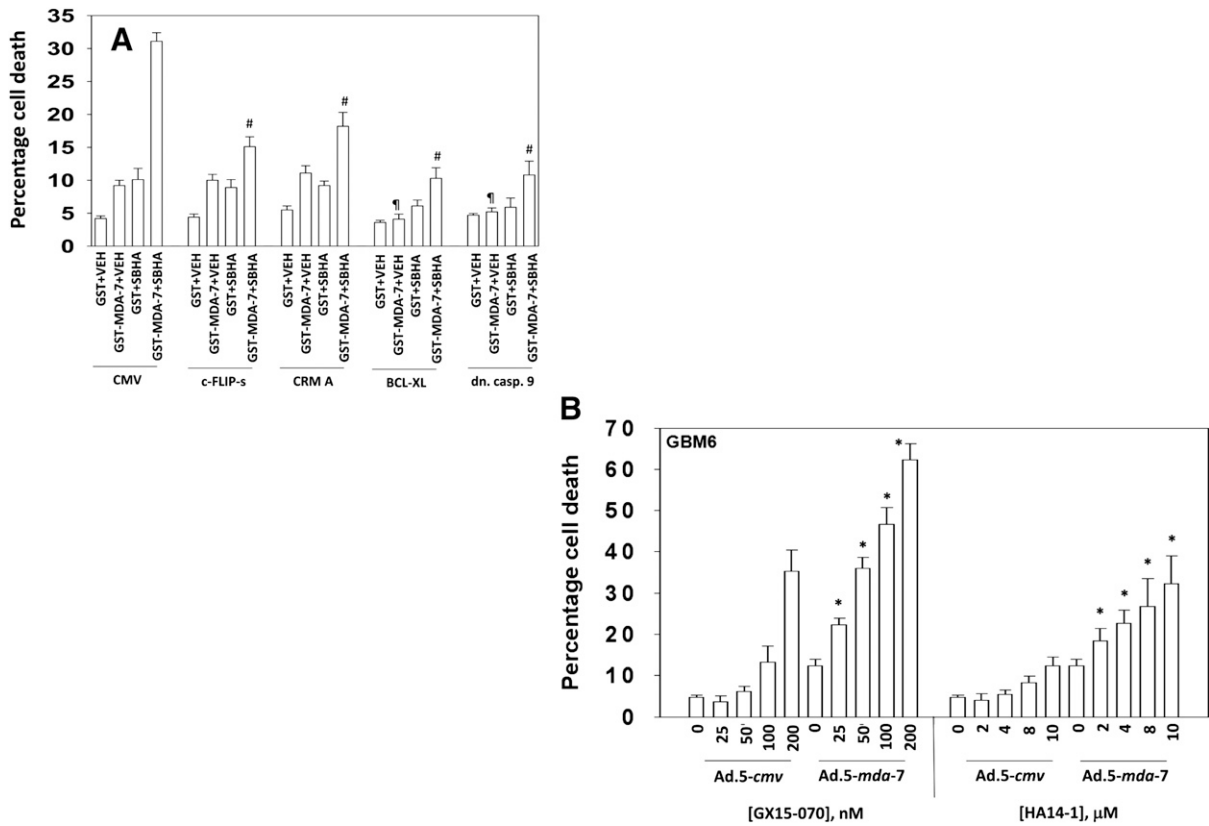
Fig. 4. SBHA intensifies and prolongs ROS and Ca^{2+} generation caused by MDA-7/IL-24. (A) GBM6 cells were infected with empty vector or recombinant serotype 5 adenovirus to express MDA-7/IL-24 at a multiplicity of infection (moi) of 10. Twenty-four hours after infection, cells were treated with vehicle (DMSO; dimethylsulfoxide) or SBHA (3 μM). Cells were loaded with DCFH (dichlorofluorescin), and the levels of ROS under each condition determined 6, 12, and 24 hours after SBHA treatment ($n = 3$, ± S.E.M.). *$P < 0.05$ greater than Ad.5-*mda*-7 + vehicle. (B) GBM6 cells were infected with empty vector or recombinant serotype 5 adenovirus to express MDA-7/IL-24 at an moi of 10. Twenty-four hours after infection, cells were treated with vehicle (DMSO) or SBHA (3 μM). Cells were loaded with Fura-2, and the levels of free Ca^{2+} under each condition were determined 6, 12, and 24 hours after SBHA treatment ($n = 3$, ± S.E.M.). *$P < 0.05$ greater than Ad.5-*mda*-7 + vehicle. (C) GBM6 cells were transfected with an empty vector plasmid, a plasmid to express thioredoxin (TRX), or a plasmid to express calbindin and in parallel infected with empty vector or recombinant serotype 5 adenovirus to express MDA-7/IL-24 at an moi of 10. Twenty-four hours after infection, cells were treated with vehicle (DMSO) or SBHA (3 μM). Cells were isolated 48 hours later, and viability was determined by trypan blue exclusion ($n = 3$, ± S.E.M.). #$P < 0.05$ less than corresponding value in CMV transfected cells.

for GBM using a tropism-modified serotype 5/3 adenovirus that conditionally replicates in tumor cells. From a rational standpoint, although our data are provocative, we do not believe, even with a conditionally replicative virus that expresses MDA-7/IL-24, that the virus as a monotherapy will have curative effects in patients. We are in the advanced stages of preparation of a phase I dose-limiting toxicity trial using Ad.5/3-PEG-E1A-*mda*-7. We believe that, in future, to truly reap benefits in GBM will require combination of virotherapy with either HDAC inhibitors or radiotherapy.

HDACIs cause oxidative damage to cells, which contributes to their lethality and possibly to the selectivity of these compounds for tumor cells (Ruefli et al., 2001; Ungerstedt et al., 2005). Our data demonstrated using Ad.5-*mda*-7 or MDA-7/IL-24 protein in GBM isolates that had been treated with several HDACIs that the combination of agents synergized to kill GBM cells. Both MDA-7/IL-24 and HDACIs increased the levels of ROS and when combined they further enhanced and prolonged ROS generation. Quenching of ROS suppressed the toxic interaction between the agents. In GBM

cells, MDA-7/IL-24 toxicity has been associated with activation of PERK and the induction of autophagy (Yacoub et al., 2008a, 2010a; Hamed et al., 2010). HDACIs enhanced both MDA-7/IL-24–induced activation of PERK and the increase in autophagy levels. HDACIs as single agents are known to cause an endoplasmic reticulum (ER) stress response that has been linked to acetylation of GRP78/BiP (Kahali et al., 2010); one portion of the mechanism by which MDA-7/IL-24 induces ER stress is through binding to GRP78/BiP (Gupta et al., 2006a,b). Further studies will be needed to determine whether GRP78/BiP is a key player in the interaction between MDA-7/IL-24 and HDACIs. Expression of dominant negative PERK or knock down of Beclin1 blocked the increase in autophagy levels and the toxic interaction between MDA-7/IL-24 and HDACIs. HDACIs downregulate c-FLIP-s levels and increase the levels of death receptors (Emanuele et al., 2007). Inhibition of the extrinsic pathway did not block MDA-7/IL-24 toxicity, but inhibition of this pathway blunted the interaction between MDA-7/IL-24 and HDACIs. We have previously shown in renal and ovarian cancer cells that MDA-7/IL-24 lethality depends

Fig. 5. SBHA enhances MDA-7/IL-24 toxicity through the extrinsic pathway. (A) GBM6 cells were infected with empty vector or recombinant serotype 5 adenovirus to express c-FLIP-s, CRM-A, BCL-XL, or dominant negative caspase 9. Twenty-four hours after infection cells were treated with GST or GST-MDA-7 (20 nM) and/or SBHA (3 μM). Cells were isolated 48 hours later and viability determined by trypan blue exclusion ($n = 3$, $\pm$ S.E.M.). [#]$P < 0.05$ less than corresponding value in CMV infected cells; [¶]$P < 0.05$ less than corresponding values in CMV, c-FLIP-s and CRM-A infected cells. (B) GBM6 cells were infected with empty vector or recombinant serotype 5 adenovirus to express MDA-7/IL-24; at a multiplicity of infection (moi) of 10. Twenty-four hours after infection cells were treated with increasing concentrations of obatoclax [GX15-070 (obatoclax), 0–200 nM] or HA14-1 (0–10 μM). Cells were isolated 24 hours later and viability determined by trypan blue exclusion ($n = 3$, $\pm$ S.E.M.). [*]$P < 0.05$ greater than corresponding Ad.5-*cmv* values.

on death receptor signaling (Park et al., 2009; Yacoub et al., 2010b). Inhibition of the intrinsic pathway blocked both MDA-7/IL-24 and HDACI lethality.
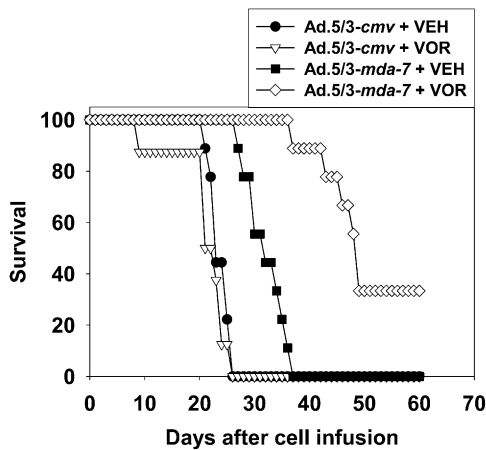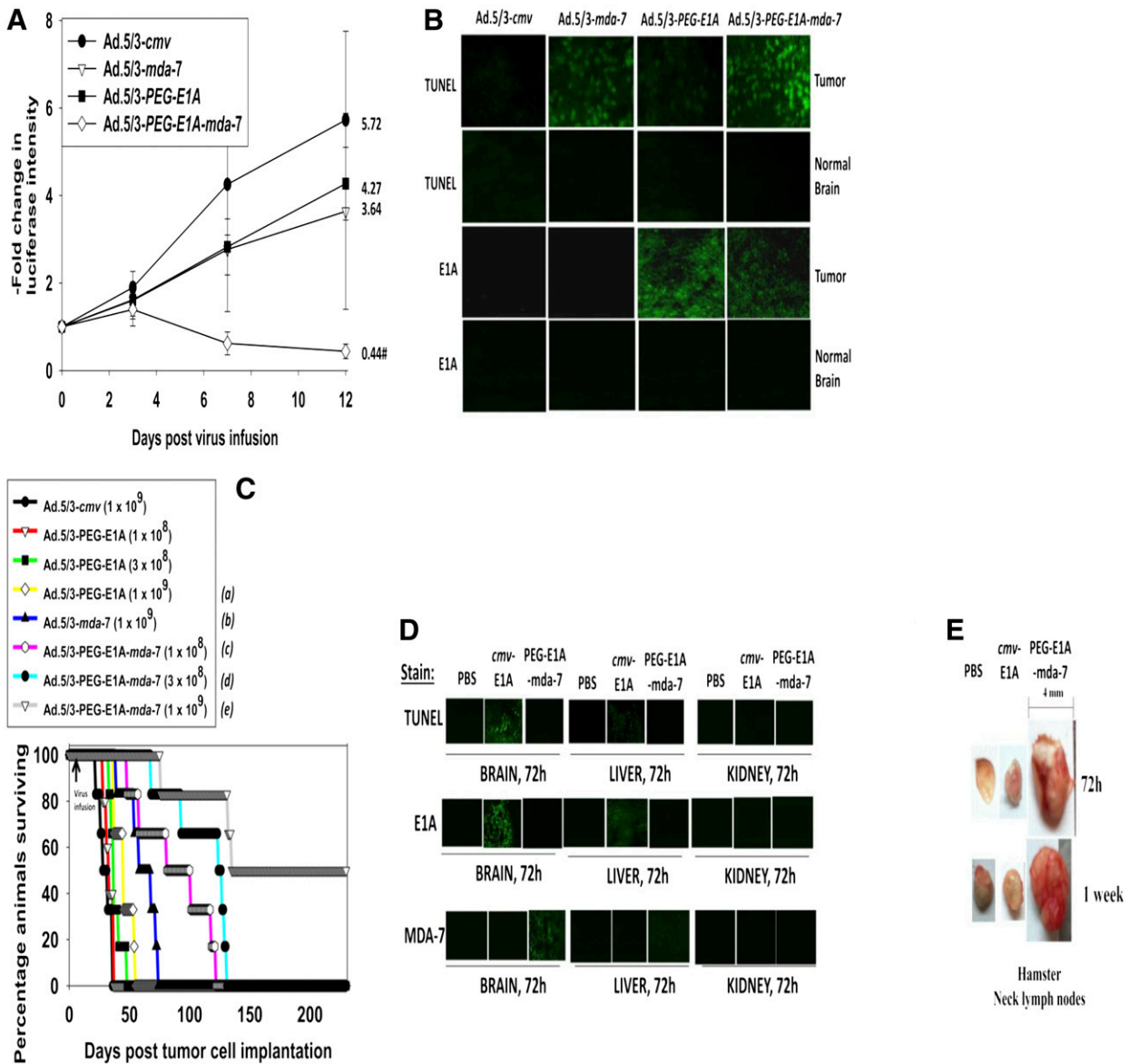

Fig. 6. SAHA enhances MDA-7/IL-24 toxicity in vivo. GBM6 cells (0.5 × 10^6) were implanted into the brains of athymic mice. Seven days later, the tumors were infused with 1 × 10^8 pfu of either Ad.5/3-*cmv* or Ad.5/3-*mda*-7. Twenty-four hours after virus infusion, the animals were treated with vehicle (VEH) diluent (cremophore, PO) or vorinostat (VOR) (SAHA, 25 mg/kg each day, PO) for 5 days. Animal survival was monitored on a daily basis ($n = 2$, eight animals total).

Several HDACIs can cross the blood-brain barrier, including sodium valproate and vorinostat (Friday et al., 2012). In vivo we noted in mice carrying GBM tumors that Ad.5/3-*mda*-7 prolonged animal survival and that this effect was augmented by HDACI treatment. There have been multiple phase I and phase II trials of HDACIs in glioma patients (Galanis et al., 2009; Chinnaiyan et al., 2012; Friday et al., 2012; Lee et al., 2012). Alone, although it is well tolerated by patients, vorinostat has modest single-agent activity in GBM, which is in agreement with our findings. Vorinostat has been combined with ionizing radiation, temozolomide, bortezomib, and bevacizumab and CPT-11 (camptothecin-11) in GBM patients, with some partial responses evident (Galanis et al., 2009; Chinnaiyan et al., 2012; Friday et al., 2012; Lee et al., 2012).

GBM was one of the earliest malignancies considered amenable to viral delivery of genetic-based therapeutics (Curiel and Fisher, 2012). Serotype 5 adenoviruses infect through the CAR, a protein whose expression is reduced in GBM cells (Paul et al., 2008; Dash et al., 2010a,b; Hamed et al., 2010; Curiel and Fisher, 2012). This has resulted in groups using targeting strategies to enhance viral infectivity via CAR-independent pathways. Several laboratories have modified the infective viral capsid "knob" to bind surface integrin proteins (an RGD modification) or by insertion into the knob of multiple lysine residues (a pK7 modification) that permit virus attachment to cells through an electrostatic

Fig. 7. Ad.5/3-PEG-E1A-*mda*-7 (Ad.5/3-*CTV*) prolongs animal survival in a dose-dependent fashion and does so to a greater extent than Ad.5/3-*mda*-7. (A) GBM6-luciferase cells (0.5×10^6) were implanted into the brains of athymic mice. Seven days later, the tumors were infused with 1×10^8 pfu of Ad.5/3-*cmv*, Ad.5/3-*mda*-7, Ad.5/3-PEG-E1A, or Ad.5/3-PEG-E1A-*mda*-7 (Ad.5/3-*CTV*). On the days indicated in the graph, the animals were injected with luciferin (150 mg/kg) and were imaged 15 minutes later after placement into an IVIS Xenogen imager (PerkinElmer, Waltham, MA). The fold increase in luciferase intensity for the mean of each animal group was plotted ($n = 2$, six animals total $\pm$ S.E.M.). #$P < 0.05$ less than Ad.5/3-*cmv*, Ad.5/3-*mda*-7, or Ad.5/3-PEG-E1A (Ad.5/3-*CTV*). The fold change in luciferase activity at day 12 is shown numerically. (B) Brains from animals at day 12 (panel A) were removed, fixed in OCT compound (Tissue Tek), and cryostat sectioned (Leica) as 12 μm sections. Sections from tumor tissue and normal brain were stained for apoptosis (TUNEL) and for expression of the viral E1A protein. (C) GBM6 cells (0.5×10^6) were implanted into the brains of athymic mice. Seven days later, the tumors were infused with Ad.5/3-*cmv* (1×10^9 pfu), Ad.5/3-*mda*-7 (1×10^9 pfu), Ad.5/3-PEG-E1A (1×10^8; 3×10^8; 1×10^9 pfu), and Ad.5/3-PEG-E1A-*mda*-7 (Ad.5/3-*CTV*) (1×10^8; 3×10^8; 1×10^9 pfu). Animal survival was monitored on a daily basis ($n = 2$, six animals total). [a]$P < 0.04$ greater survival than Ad.5/3-*cmv*; [b]$P < 0.0008$ greater survival than Ad.5/3-*cmv*; [c]$P < 0.04$ greater survival than Ad.5/3-*mda*-7; [d]$P < 0.004$ greater survival than Ad.5/3-*mda*-7; [e]$P < 0.0008$ greater survival than Ad.5/3-PEG-E1A-*mda*-7 (Ad.5/3-*CTV*) at a dose of 3×10^8 pfu. (D) Syrian hamster brains were infused with PBS, Ad.5/3-*cmv*-E1A (2×10^9 pfu), or Ad.5/3-PEG-E1A-*mda*-7 (Ad.5/3-*CTV*) (2×10^9 pfu). Seventy-two hours after infusion, the animal brains, livers, and kidneys were isolated and fixed. Sections (12 μm) were taken and stained for apoptosis (TUNEL), the levels of viral E1A protein, and the levels of MDA-7/IL-24 protein. (E) Syrian hamster brains were infused with PBS, Ad.5/3-*cmv*-E1A (2×10^9 pfu), or Ad.5/3-PEG-E1A-*mda*-7 (Ad.5/3-*CTV*) (2×10^9 pfu). Seventy-two hours and 1 week after infusion, the animals were sacrificed, and their neck lymph nodes were dissected.

interactions (Curiel and Fisher, 2012). We have taken the infective capsid knob from a serotype 3 adenovirus and incorporated it into the adenovirus type 5 knob; we demonstrated that modified serotype 5/3 knob adenoviruses were able to achieve enhanced gene transduction into low- and high-CAR containing human GBM tumor cells (Paul et al., 2008; Hamed et al., 2010; Curiel and Fisher, 2012). We noted

that a serotype 5/3 virus was more efficient at transducing genes into GBM cells than either an RGD/double RGD modification or a pK7 modification (Hamed et al., 2010; Curiel and Fisher, 2012).

GBM is a highly invasive and diffuse tumor, which makes infection of every tumor cell a difficult and probably impossible proposition when using a nonreplicative adenovirus.

Many prior studies in GBM have used serotype 5 viruses, which as mentioned previously have reduced infectivity in CAR low GBM cells in situ. In addition to these limitations, prior gene therapy studies in GBM have also frequently expressed intracellular proteins such as p53, which will result in only those cells that have been virally infected being subjected to the actions of the therapeutic gene; that is, these infections lack a "bystander" secreted protein effect on uninfected tumor cells (Fisher, 2005; Sauane et al., 2008; Dash et al., 2010a,b; Hamed et al., 2010; Curiel and Fisher, 2012). In GBM tumors growing on the flanks of mice, Ad.5/3-mda-7 therapy suppressed the growth not only of the tumor into which it had been injected but also the tumor on the opposite flank (i.e., the uninfected tumor). Thus, consistent with other cancer indications, Ad.5/3-mda-7 generates a "bystander effect" in the contralateral uninfused GBM tumor (H. A. Hamed, P. B. Fisher, and P. Dent, unpublished observations) (Sauane et al., 2008; Park et al., 2009). Collectively these constraints may explain the relative lack of efficacy of previous gene therapy approaches in GBM.

The use of Ad.5/3-PEG-E1A-mda-7 (Ad.5/3-CTV) is one approach to overcoming the issues of infectivity and the diffuse nature of GBM. Ad.5/3-PEG-E1A-mda-7 efficiently infects low-CAR GBM cells and enhances infectivity even in high-CAR GBM cells (Hamed et al., 2010). Ad.5/3-PEG-E1A-mda-7 replicates selectively in tumor cells, which can result in virus dissemination within the brain to infect tumor cells centimeters away from the site of virus administration. MDA-7/IL-24 protein is secreted from infected GBM cells and astrocytes, and as we have recently demonstrated in GBM and renal and prostate cancer cells, media containing secreted MDA-7/IL-24 can induce apoptosis in uninfected tumor cells (Sauane et al., 2008; Park et al., 2009; Yacoub et al., 2010a; Curiel and Fisher, 2012). MDA-7/IL-24 can induce its own synthesis in tumor cells, amplifying the initial effect of viral infection/the initial MDA-7/IL-24 secretion (Sauane et al., 2008; Park et al., 2009; Curiel and Fisher, 2012). Thus, the expression of MDA-7/IL-24 overcomes the problems associated with a lack of a "bystander" effect after gene therapeutic intervention.

In a dose-dependent fashion, Ad.5/3-PEG-E1A-mda-7 increased animal survival when compared with Ad.5/3-mda-7. At the highest virus dose tested, Ad.5/3-PEG-E1A-mda-7 prolonged the survival of some animals to >250 days. No change in animal behavior or body mass was noted with these interventions. These data argue that Ad.5/3-PEG-E1A-mda-7 is a safe and efficacious virus for the treatment of animal GBM models. Based on these findings, as suggested to us by the U.S. FDA, we performed preliminary toxicology testing using an approved rodent model for human adenovirus replication, the Syrian hamster (Curiel and Fisher, 2012; Dhar et al., 2012). Infusion into the hamster brain of a constitutively replicating adenovirus Ad.5/3-cmv-E1A resulted in significant levels of apoptosis and expression of the viral protein E1A; thus, viral replication had occurred.

The liver is a major site of adenovirus clearance from the blood; after infusion of this virus into the brain, we noted low levels of apoptosis and E1A expression in the liver. The kidneys did not exhibit any virus uptake. Infusion into the brain of Ad.5/3-PEG-E1A-mda-7 did not result in apoptosis or expression of the viral E1A protein. This argues that control of virus replication by the PEG-3 promoter was tumor-cell

specific. Syrian hamsters are an immune-competent model and would be expected to immunologically respond to virus replication (Curiel and Fisher, 2012; Dhar et al., 2012). In agreement with this hypothesis we found that neck lymph nodes were enlarged in Ad.5/3-cmv-E1A–infected animals, but infusion of Ad.5/3-PEG-E1A-mda-7 had no obvious effect on lymph node size. These findings further demonstrate that Ad.5/3-PEG-E1A-mda-7 is a safe and efficacious virus in vivo.

Our data demonstrate that HDACIs increase MDA-7/IL-24 lethality through mechanisms involving ER stress and activation of the extrinsic apoptosis pathway. Adenoviral delivery of mda-7/IL-24 to GBM cells and tumors can be enhanced by a serotype 3 tropism modification and by engineering of the virus to conditionally replicate in tumor cells.

Authorship Contributions

Participated in research design: Dent, Fisher, Grant.
Conducted experiments: Hamed, Yacoub, Park.
Contributed new reagents or analytic tools: Das, Sarkar.
Performed data analysis: Archer, Dent.
Wrote or contributed writing of the manuscript: Dent, Fisher.

References

Azab B, Dash R, Das SK, Bhutia SK, Shen XN, Quinn BA, Sarkar S, Wang XY, Hedvat M, and Dmitriev IP et al. (2012) Enhanced delivery of mda-7/IL-24 using a serotype chimeric adenovirus (Ad.5/3) in combination with the Apogossypol derivative BI-97C1 (Sabutoclax) improves therapeutic efficacy in low CAR colorectal cancer cells. *J Cell Physiol* 227:2145–2153.

Bhutia SK, Das SK, Azab B, Dash R, Su ZZ, Lee SG, Dent P, Curiel DT, Sarkar D, and Fisher PB (2011) Autophagy switches to apoptosis in prostate cancer cells infected with melanoma differentiation associated gene-7/interleukin-24 (mda-7/IL-24). *Autophagy* 7:1076–1077.

Chinnaiyan P, Chowdhary S, Potthast L, Prabhu A, Tsai YY, Sarcar B, Kahali S, Brem S, Yu HM, and Rojiani A et al. (2012) Phase I trial of vorinostat combined with bevacizumab and CPT-11 in recurrent glioblastoma. *Neuro-oncol* 14:93–100.

Cunningham CC, Chada S, Merritt JA, Tong A, Senzer N, Zhang Y, Mhashilkar A, Parker K, Vukelja S, and Richards D et al. (2005) Clinical and local biological effects of an intratumoral injection of mda-7 (IL24; INGN 241) in patients with advanced carcinoma: a phase I study. *Mol Ther* 11:149–159.

Curiel DT and Fisher PB eds. (2012) Applications of Viruses for Cancer Therapy, Advances in Cancer Research, vol 115, pp 1–334, Academic Press, Waltham, MA, ISBN: 9780123983428.

Dai Y, Rahmani M, Dent P, and Grant S (2005) Blockade of histone deacetylase inhibitor-induced RelA/p65 acetylation and NF-κB activation potentiates apoptosis in leukemia cells through a process mediated by oxidative damage, XIAP downregulation, and c-Jun N-terminal kinase 1 activation. *Mol Cell Biol* 25:5429–5444.

Dash R, Bhutia SK, Azab B, Su ZZ, Quinn BA, Kegelmen TP, Das SK, Kim K, Lee SG, and Park MA et al. (2010a) mda-7/IL-24: a unique member of the IL-10 gene family promoting cancer-targeted toxicity. *Cytokine Growth Factor Rev* 21:381–391.

Dash R, Azab B, Quinn BA, Shen X, Wang XY, Das SK, Rahmani M, Wei J, Hedvat M, and Dent P et al. (2011) Apogossypol derivative BI-97C1 (Sabutoclax) targeting Mcl-1 sensitizes prostate cancer cells to mda-7/IL-24-mediated toxicity. *Proc Natl Acad Sci USA* 108:8785–8790.

Dash R, Dmitriev I, Su ZZ, Bhutia SK, Azab B, Vozhilla N, Yacoub A, Dent P, Curiel DT, and Sarkar D et al. (2010b) Enhanced delivery of mda-7/IL-24 using a serotype chimeric adenovirus (Ad.5/3) improves therapeutic efficacy in low CAR prostate cancer cells. *Cancer Gene Ther* 17:447–456.

Dhar D, Toth K, and Wold WS (2012) Syrian hamster tumor model to study oncolytic Ad5-based vectors. *Methods Mol Biol* 797:53–63.

Dent P, Yacoub A, Hamed HA, Park MA, Dash R, Bhutia SK, Sarkar D, Wang XY, Gupta P, and Emdad L et al. (2010a) The development of MDA-7/IL-24 as a cancer therapeutic. *Pharmacol Ther* 128:375–384.

Dent P, Yacoub A, Hamed HA, Park MA, Dash R, Bhutia SK, Sarkar D, Gupta P, Emdad L, and Lebedeva IV et al. (2010b) MDA-7/IL-24 as a cancer therapeutic: from bench to bedside. *Anticancer Drugs* 21:725–731.

Ekmekcioglu S, Ellerhorst J, Mhashilkar AM, Sahin AA, Read CM, Prieto VG, Chada S, and Grimm EA (2001) Down-regulated melanoma differentiation associated gene (mda-7) expression in human melanomas. *Int J Cancer* 94:54–59.

Ellerhorst JA, Prieto VG, Ekmekcioglu S, Broemeling L, Yekell S, Chada S, and Grimm EA (2002) Loss of MDA-7 expression with progression of melanoma. *J Clin Oncol* 20:1069–1074.

Ellis L and Pili R (2010) Histone deacetylase inhibitors: advancing therapeutic strategies in hematological and solid malignancies. *Pharmaceuticals (Basel)* 3: 2411–2469.

Emanuele S, Lauricella M, Carlisi D, Vassallo B, D'Anneo A, Di Fazio P, Vento R, and Tesoriere G (2007) SAHA induces apoptosis in hepatoma cells and

synergistically interacts with the proteasome inhibitor Bortezomib. *Apoptosis* **12**: 1327–1338.

Emdad L, Lebedeva IV, Su ZZ, Gupta P, Sauane M, Dash R, Grant S, Dent P, Curiel DT, and Sarkar D et al. (2009) Historical perspective and recent insights into our understanding of the molecular and biochemical basis of the antitumor properties of mda-7/IL-24. *Cancer Biol Ther* **8**:391–400.

Fisher PB, Gopalkrishnan RV, Chada S, Ramesh R, Grimm EA, Rosenfeld MR, Curiel DT, and Dent P (2003) *mda-7*/IL-24, a novel cancer selective apoptosis inducing cytokine gene: from the laboratory into the clinic. *Cancer Biol Ther* **2**(Suppl 1)S23–S37.

Fisher PB (2005) Is *mda-7*/IL-24 a "magic bullet" for cancer? *Cancer Res* **65**: 10128–10138.

Frew AJ, Johnstone RW, and Bolden JE (2009) Enhancing the apoptotic and therapeutic effects of HDAC inhibitors. *Cancer Lett* **280**:125–133.

Friday BB, Anderson SK, Buckner J, Yu C, Giannini C, Geoffroy F, Schwerkoske J, Mazurczak M, Gross H, and Pajon E et al. (2012) Phase II trial of vorinostat in combination with bortezomib in recurrent glioblastoma: a north central cancer treatment group study. *Neuro-oncol* **14**:215–221.

Galanis E, Jaeckle KA, Maurer MJ, Reid JM, Ames MM, Hardwick JS, Reilly JF, Loboda A, Nebozhyn M, and Fantin VR et al. (2009) Phase II trial of vorinostat in recurrent glioblastoma multiforme: a north central cancer treatment group study. *J Clin Oncol* **27**:2052–2058.

Gupta P, Su ZZ, Lebedeva IV, Sarkar D, Sauane M, Emdad L, Bachelor MA, Grant S, Curiel DT, and Dent P et al. (2006a) *mda-7*/IL-24: multifunctional cancer-specific apoptosis-inducing cytokine. *Pharmacol Ther* **111**:596–628.

Gupta P, Walter MR, Su ZZ, Lebedeva IV, Emdad L, Randolph A, Valerie K, Sarkar D, and Fisher PB (2006b) BiP/GRP78 is an intracellular target for MDA-7/IL-24 induction of cancer-specific apoptosis. *Cancer Res* **66**:8182–8191.

Hamed HA, Yacoub A, Park MA, Eulitt PJ, Dash R, Sarkar D, Dmitriev IP, Lesniak MS, Shah K, and Grant S et al. (2010) Inhibition of multiple protective signaling pathways and Ad.5/3 delivery enhances mda-7/IL-24 therapy of malignant glioma. *Mol Ther* **18**:1130–1142.

Jiang H, Lin JJ, Su ZZ, Goldstein NI, and Fisher PB (1995) Subtraction hybridization identifies a novel melanoma differentiation associated gene, *mda-7*, modulated during human melanoma differentiation, growth and progression. *Oncogene* **11**: 2477–2486.

Kahali S, Sarcar B, Fang B, Williams ES, Koomen JM, Tofilon PJ, and Chinnaiyan P (2010) Activation of the unfolded protein response contributes toward the antitumor activity of vorinostat. *Neoplasia* **12**:80–86.

Lebedeva IV, Sauane M, Gopalkrishnan RV, Sarkar D, Su ZZ, Gupta P, Nemunaitis J, Cunningham C, Yacoub A, and Dent P et al. (2005) *mda-7*/IL-24: exploiting cancer's Achilles' heel. *Mol Ther* **11**:4–18.

Lee EQ, Puduvalli VK, Reid JM, Kuhn JG, Lamborn KR, Cloughesy TF, Chang SM, Drappatz J, Yung WK, and Gilbert MR et al. (2012) Phase I study of vorinostat in combination with temozolomide in patients with high-grade gliomas: North American Brain Tumor Consortium Study 04-03. *Clin Cancer Res* **18**:6032–6039.

Park MA, Walker T, Martin AP, Allegood J, Vozhilla N, Emdad L, Sarkar D, Rahmani M, Graf M, and Yacoub A et al. (2009) MDA-7/IL-24-induced cell killing in malignant renal carcinoma cells occurs by a ceramide/CD95/PERK-dependent mechanism. *Mol Cancer Ther* **8**:1280–1291.

Paul CP, Everts M, Glasgow JN, Dent P, Fisher PB, Ulasov IV, Lesniak MS, Stoff-Khalili MA, Roth JC, and Preuss MA et al. (2008) Characterization of infectivity of knob-modified adenoviral vectors in glioma. *Cancer Biol Ther* **7**:786–793.

Robins HI, Chang S, Butowski N, and Mehta M (2007) Therapeutic advances for glioblastoma multiforme: current status and future prospects. *Curr Oncol Rep* **9**: 66–70.

Rosato RR and Grant S (2004) Histone deacetylase inhibitors in clinical development. *Expert Opin Investig Drugs* **13**:21–38.

Ruefli AA, Ausserlechner MJ, Bernhard D, Sutton VR, Tainton KM, Kofler R, Smyth MJ, and Johnstone RW (2001) The histone deacetylase inhibitor and chemotherapeutic agent suberoylanilide hydroxamic acid (SAHA) induces a cell-death pathway characterized by cleavage of Bid and production of reactive oxygen species. *Proc Natl Acad Sci USA* **98**:10833–10838.

Sarkar D, Lebedeva IV, Su ZZ, Park ES, Chatman L, Vozhilla N, Dent P, Curiel DT, and Fisher PB (2007) Eradication of therapy-resistant human prostate tumors using a cancer terminator virus. *Cancer Res* **67**:5434–5442.

Sarkar D, Su ZZ, Park ES, Vozhilla N, Dent P, Curiel DT, and Fisher PB (2008) A cancer terminator virus eradicates both primary and distant human melanomas. *Cancer Gene Ther* **15**:293–302.

Sarkar D, Su ZZ, Vozhilla N, Park ES, Gupta P, and Fisher PB (2005) Dual cancer-specific targeting strategy cures primary and distant human breast carcinomas in nude mice. *Proc Natl Acad Sci USA* **102**:14034–14039.

Sauane M, Su ZZ, Dash R, Liu X, Norris JS, Sarkar D, Lee SG, Allegood JC, Dent P, and Spiegel S et al. (2010) Ceramide plays a prominent role in MDA-7/IL-24-induced cancer-specific apoptosis. *J Cell Physiol* **222**:546–555.

Sauane M, Su ZZ, Gupta P, Lebedeva IV, Dent P, Sarkar D, and Fisher PB (2008) Autocrine regulation of mda-7/IL-24 mediates cancer-specific apoptosis. *Proc Natl Acad Sci USA* **105**:9763–9768.

Spiegel S, Milstien S, and Grant S (2012) Endogenous modulators and pharmacological inhibitors of histone deacetylases in cancer therapy. *Oncogene* **31**:537–551.

Su Z, Lebedeva IV, Gopalkrishnan RV, Goldstein NI, Stein CA, Reed JC, Dent P, and Fisher PB (2001) A combinatorial approach for selectively inducing programmed cell death in human pancreatic cancer cells. *Proc Natl Acad Sci USA* **98**: 10332–10337.

Su ZZ, Madireddi MT, Lin JJ, Young CS, Kitada S, Reed JC, Goldstein NI, and Fisher PB (1998) The cancer growth suppressor gene *mda-7* selectively induces apoptosis in human breast cancer cells and inhibits tumor growth in nude mice. *Proc Natl Acad Sci USA* **95**:14400–14405.

Su ZZ, Sarkar D, Emdad L, Duigou GJ, Young CS, Ware J, Randolph A, Valerie K, and Fisher PB (2005) Targeting gene expression selectively in cancer cells by using the progression-elevated gene-3 promoter. *Proc Natl Acad Sci USA* **102**: 1059–1064.

Tang Y, Yacoub A, Hamed HA, Poklepovic A, Tye G, Grant S, and Dent P (2012) Sorafenib and HDAC inhibitors synergize to kill CNS tumor cells. *Cancer Biol Ther* **13**:567–574.

Ungerstedt JS, Sowa Y, Xu WS, Shao Y, Dokmanovic M, Perez G, Ngo L, Holmgren A, Jiang X, and Marks PA (2005) Role of thioredoxin in the response of normal and transformed cells to histone deacetylase inhibitors. *Proc Natl Acad Sci USA* **102**: 673–678.

Yacoub A, Hamed HA, Allegood J, Mitchell C, Spiegel S, Lesniak MS, Ogretmen B, Dash R, Sarkar D, and Broaddus WC et al. (2010a) PERK-dependent regulation of ceramide synthase 6 and thioredoxin play a key role in mda-7/IL-24-induced killing of primary human glioblastoma multiforme cells. *Cancer Res* **70**:1120–1129.

Yacoub A, Park MA, Gupta P, Rahmani M, Zhang G, Hamed H, Hanna D, Sarkar D, Lebedeva IV, and Emdad L et al. (2008a) Caspase-, cathepsin-, and PERK-dependent regulation of MDA-7/IL-24-induced cell killing in primary human glioma cells. *Mol Cancer Ther* **7**:297–313.

Yacoub A, Gupta P, Park MA, Rhamani M, Hamed H, Hanna D, Zhang G, Sarkar D, Lebedeva IV, and Emdad L et al. (2008b) Regulation of GST-MDA-7 toxicity in human glioblastoma cells by ERBB1, ERK1/2, PI3K, and JNK1-3 pathway signaling. *Mol Cancer Ther* **7**:314–329.

Yacoub A, Hamed H, Emdad L, Dos Santos W, Gupta P, Broaddus WC, Ramakrishnan V, Sarkar D, Shah K, and Curiel DT et al. (2008c) MDA-7/IL-24 plus radiation enhance survival in animals with intracranial primary human GBM tumors. *Cancer Biol Ther* **7**:917–933.

Yacoub A, Liu R, Park MA, Hamed HA, Dash R, Schramm DN, Sarkar D, Dimitriev IP, Bell JK, and Grant S et al. (2010b) Cisplatin enhances protein kinase R-like endoplasmic reticulum kinase- and CD95-dependent melanoma differentiation-associated gene-7/interleukin-24-induced killing in ovarian carcinoma cells. *Mol Pharmacol* **77**:298–310.

Address correspondence to: Dr. Paul Dent, Department of Neurosurgery, 401 College Street, Massey Cancer Center, Room 280a, Box 980035, Virginia Commonwealth University, Richmond, VA 23298-0035. E-mail: pdent@vcu.edu